Riding simulators: What is the way forward?

Citation for the original published paper (version of record):

Dozza, M., Li, T., Bruzelius, F. (2026). Riding simulators: What is the way forward?. Transportation Research Part F: Traffic Psychology and Behaviour, 122. http://dx.doi.org/10.1016/j.trf.2026.103739

Transportation Research Part F: Psychology and Behaviour 122 (2026) 103739

Contents lists available at ScienceDirect

Transportation Research Part F: Psychology and Behaviour

journal homepage: www.elsevier.com/locate/trf

Riding simulators: What is the way forward?

Marco Dozza *, Tianyou Li, Fredrik Bruzelius

Chalmers University of Technology, Mechanical Engineering Department, Hörsalvägen 7A (Campus Johanneberg, M-building 3rd floor), SE-412 58 Göteborg, Sweden

A R T I C L E I N F O

Keywords:
Riding simulator
Virtual environment
Vehicle dynamics
Balance
Bicycles
E-scooters
Micromobility vehicles
Motion analysis
Obstacle avoidance
Lateral control

A B S T R A C T

This paper introduces a novel micromobility simulator that combines a large treadmill with stereophotogrammetry to enable virtual testing of real bicycles and e-scooters while preserving the balancing task and allowing lateral maneuvering. Unlike existing riding simulators, the platform accommodates real vehicles, increasing ecological validity for research on balance and control. The simulator architecture is presented and its potential demonstrated by comparing lateral control during obstacle avoidance—a critical task that previous simulators could not address with comparable realism.

Because full balance control is preserved, we propose new metrics for comparing balance across micromobility vehicles and show how they complement traditional indicators of lateral control and performance. Overall, the paper contributes 1) a vehicle-agnostic riding simulator and 2) a minimal yet discriminative set of indicators for maneuvering and balance across tasks and vehicles.

Twelve participants performed cruising and obstacle-avoidance tasks at different speeds on both a bicycle and an e-scooter. Four indicators were analyzed: standard deviation of lane position and steering angle, adapted from driving simulation research, and standard deviation of lean angle and relative upper–lower body angle, inspired by motor control literature. Results revealed distinct patterns across tasks, speeds, and vehicles, with low redundancy among indicators. Notably, during obstacle avoidance, participants exhibited different postural strategies on bicycles and e-scooters and collided more frequently when cycling.

The simulator enables new research on human–vehicle interaction, ergonomics, and safety in micromobility, although further validation and enhancements are needed to fully exploit its potential.

1. Introduction

For the last two decades, driving simulators have supported the development of advanced driving and assistance systems (ADAS) by enabling repeated exposure to critical situations under controlled and safe conditions. For instance, driving simulators have been used to design warning systems and identify which human–machine interface (HMI) configurations elicit the safest reactions (Weir, 2010). They have also exposed drivers to low-friction scenarios to evaluate responses to different stability control systems (Markkula et al., 2013). More recently, driving simulators have contributed to research on L1–L3 automation in numerous experiments (Merat et al., 2014; Morando et al., 2021). Because simulators can be networked, multiple participants can share the same virtual environment,

* Corresponding author at: Division of Vehicle Safety, Sweden.
E-mail address: marco.dozza@chalmers.se (M. Dozza).

https://doi.org/10.1016/j.trf.2026.103739
Received 9 January 2026; Received in revised form 13 July 2026; Accepted 13 July 2026
Available online 27 July 2026
1369-8478/

enabling studies of driver interactions and improving ecological validity.

Simulators that allow road users to interact in virtual traffic environments have been developed for various vehicle types—and even for pedestrians. For instance, the Hiker platform enables pedestrians to negotiate intersections with automated vehicles (AVs) or human-driven vehicles in remote but connected simulators (Lyu et al., 2024). Such setups are critical for developing vehicle automation, as safe interaction with vulnerable road users remains one of the greatest challenges for AVs in urban environments (Sandt & Owens, 2017). In this context, interactions with micromobility vehicles (e.g., bicycles and e-scooters) pose a significant challenge for urban automation (Mohammadi et al., 2023). However, riding simulators are still limited in availability and development, partly because they are more complex to design than driving simulators.

The balancing task—essential for most micromobility vehicles—introduces unique technical challenges in the design of riding simulator. Several bicycle simulators have been proposed, each making trade-offs between preserving balance and enabling maneuverability. For example, the unique bicycle simulator at VTI, the Swedish National Road Transport Research Institute, (Ochel et al., 2025) Fig. 1A, uses rollers to fully preserve balance but severely restricts steering and, of course, braking. Much more commons are simulators such as the one at WIVW, the Würzburg Institute for Traffic Sciences, (Stemmler et al., 2024) that allow free steering and braking but largely eliminate the balancing task, Fig. 1B. Similar stationary simulators can be found at several other institutions: University of Lund (Jafari et al., 2025); University of Ingolstadt (Von Sawitzky et al., 2022), Gustave Eiffel University (Shoman & Imine, 2021), University of Iowa (Plumert et al., 2010), and Monash (O'Hern & Estgfaeller, 2020) just to mention a few. Some of these simulators, although static, incorporate balance in the virtual environment without replicating its physical dynamics (Dialynas et al., 2019), though the ecological validity of this method may be questionable. A recent inventive simulator from Delft University of Technology actively controls a stationary bicycle using three independent motors and a dynamic model, requiring riders to perform the balancing task realistically (Sporrel et al., 2025); Fig. 1C. If cycling simulators are limited, scooter simulators are even less developed and remain in their infancy largely inspired by the design of static bicycle simulators (Christoforou et al., 2026; MicroVRide, 2025). Critically, there is no consensus on which simulator configurations are appropriate for specific research questions or what level of realism, particularly regarding balance, is necessary to ensure valid results, especially when investigating interactions among road users.

Several performance indicators for lateral maneuvering have been established for driving simulators. For example, standard deviation of lane position (SDLP) and steering angle (SDSA) are widely used to assess lateral control for driving (Bowers et al., 2010; Hildreth et al., 2000; Louwerens et al., 1987). These indicators could be adapted for riding simulators, but new metrics are needed to capture balancing performance and fully evaluate rider behavior in micromobility contexts. In this regard, literature on motor control and balance may offer more relevant insights than motor-vehicle research. For instance, studies have examined how humans adjust their center of mass (Pai & Patton, 1997) and employ multi-segment strategies to maintain balance (Horak & Nashner, 1986).

In this paper, we present a new platform for virtual micromobility testing that: (1) accommodates commercial and prototypical micromobility vehicles with human riders, (2) preserves the balancing task, and (3) allows lateral maneuvering. We also report reference values for lateral-control indicators adapted from driving simulator research and introduce new metrics addressing balance in different tasks requiring lateral control. Finally, we compare obstacle avoidance performances across e-scooter riding and cycling,

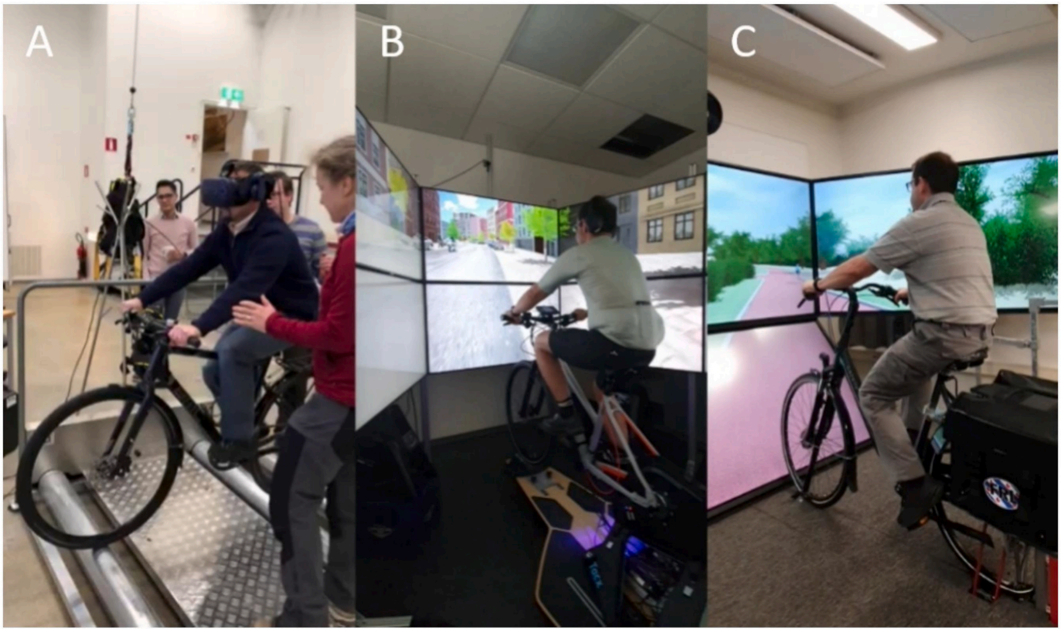

Fig. 1. – Examples of different riding simulators. A: VTI, Linköping, Sweden; B: WIVW Wurzburg, Germany; C: University of Gröningen, The Netherlands. Play the supplementary video S1 to see them in motion.

illustrating an analysis that—at present—can only be achieved using our simulator by leveraging the flexibility, repeatability, and safety of our virtual environment. Thus, the primary contribution of this paper is methodological, aiming to inform future directions in the development of riding simulators.

2. Methods

We combined a motion analysis system with a large treadmill so that riders could perform different riding tasks in a virtual environment with different micromobility vehicles (Fig. 2).

2.1. Apparatus

2.1.1. Hardware

Participants rode on a treadmill measuring 3.5 m in length and 2.5 m in width (Rodby RL3500E). The treadmill speed was adjustable between 2 and 50 km/h with 1% precision. Surrounding the treadmill, 12 Qualisys Miqus M3 cameras recorded motion at 300 fps, tracking passive markers with sub-millimetric accuracy. A 65-in. display was positioned at the rider's eye level to render the virtual environment (Fig. 2).

2.1.2. Software

Two separate computers controlled the treadmill and the motion analysis system, running Rodby and Qualisys commercial software, respectively. The Qualisys computer also hosted a custom Unreal Engine interface that processed motion data in real time to render a virtual environment based on the rider's and vehicle's movements on the treadmill. The virtual scene displayed a straight road advancing at the same speed as the treadmill, creating the illusion of forward motion (Fig. 3). Head-tracking data from the motion analysis systems adjusted the viewpoint according to the rider's estimated head facing direction, while vehicle kinematics, again from the motion analysis system, controlled lateral displacement in the virtual world. Depending on the task, the environment included obstacles, lane markings, and visual cues such as color-coded arrows to guide participants.

2.2. Experiment

Twelve participants (6 female and 6 male; age: 26.7 ± 3.4 years; height: 1.74 ± 0.10 m; weight: 66.7 ± 15.0 kg) rode on the treadmill after providing informed consent. The study was approved by the National Board of Ethics (Ref. 2024–03368-01). Eligibility criteria required that participants had no pathologies affecting mobility, had not experienced serious traffic accidents during their lifetime, and were able to ride both vehicles. All participants reported being more familiar with cycling than with e-scootering in their daily activities. Nevertheless, all had prior experience with both cycling and e-scootering and completed practice sessions on the treadmill using both vehicles before the experiment began Participants completed three riding tasks: (1) cruising, (2) lane centering, and (3) obstacle avoidance (Fig. 3). In the cruising task, participants rode an e-scooter (*E*-Wheels E2S) and a bicycle (TREK FX1) without specific instructions on lateral control (Fig. 3A). In the lane-centering task, riders were instructed to stay as close as possible to the center line, aided by an on-screen arrow that turned green when centered and gradually shifted to red as they drifted left or right (Fig. 3B). In the obstacle-avoidance task, participants maneuvered around virtual concrete blocks by periodically moving to the far left and right of the treadmill (Fig. 3C). To avoid the participants could just tune to an easily predictable behavior, the distance between the obstacles was randomized within the intervals 6–12 m and 14–21 m for 6 km/h and 20 km/h, respectively.

To prevent falls, vehicles were secured to a linear bearing that allowed free lateral movement while preventing backward displacement. Participants wore a safety harness connected to an emergency stop (Fig. 2), and a second emergency-stop button was accessible to the experimenter. Half of the participants started with the bicycle and half with the e-scooter. Cruising and obstacle-avoidance tasks were performed at two speeds (6 and 20 km/h), while lane centering was only at 6 km/h. Trial durations were 35 s for cruising, 125 s for obstacle avoidance, and 65 s for lane centering. Each participant completed seven randomized trials per vehicle. Motion capture was enabled by passive markers (12 on each vehicle and 41 on each participant), allowing detailed recording of human and vehicle kinematics. The motion capture system was calibrated following the Qualisys protocol to ensure marker detection with sub-millimeter accuracy. In addition, an individualized skeletal model was created for each participant prior to the experiment to

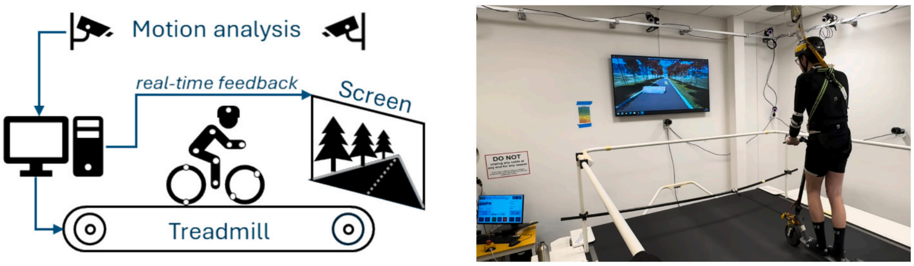

Fig. 2. – Experimental apparatus (left). Photo from one of the experiments with an e-scooter (play the supplementary video S2 to see it in motion).

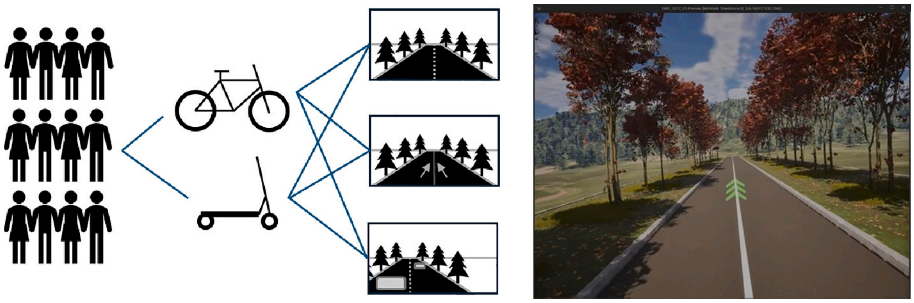

Fig. 3. – Experimental set-up, play the supplementary video S3 to see the tasks in motion in the virtual world.

facilitate marker reconstruction during post-processing. At the end of the experiment, participants rated the realism of the simulator using a Likert scale (0–7), assessing both the overall experience and specific tasks, including lane keeping and obstacle avoidance.

2.3. Analysis

Motion analysis data were labeled and sanitized to generate skeletal and vehicle models (Fig. 4). Motion analysis data processing consisted of preprocessing and smoothing steps. During preprocessing, markers were first labeled in QTM to enable execution of the skeleton solver. Marker trajectories were then visually inspected to ensure the absence of gaps or mislabeling. Any gaps identified were filled using relational gap-filling techniques, and ghost markers were removed. Smoothing was performed by applying a fourth-order Butterworth low-pass filter with a 10-Hz cutoff frequency to the marker trajectories to reduce noise. By integrating participant and vehicle weights, human body models, and vehicle geometry with these models, we computed four performance indicators: two describing lateral control and two specifically targeting the balancing task (Fig. 4). A key step in this process was creating a custom human body model in OpenSim (Delp et al., 2007) by combining the Qualisys model Gait2392 with the Rajagopal arm model (Rajagopal et al., 2016).

2.3.1. Performance indicators for lateral control

We calculated the standard deviation of lane position (SDLP) based on the lateral movement of the wheelbase midpoint projected onto the treadmill. Similarly, we computed the standard deviation of the steering angle (SDSA). Both indicators were adapted from established metrics in driving simulator research.

2.3.2. Performance indicators for balancing

Using OpenSim, we combined the center of mass (COM) of each human body segment with that of the vehicle to estimate the overall system COM. We also calculated the COM for the upper and lower body separately. The lean angle of the rider–vehicle system was defined as the roll of the overall COM around the wheelbase axis, and its standard deviation (SDLA) served as one performance indicator for the balancing task. On the same plane, we computed the relative angle between the upper and lower body, using its standard deviation (SDRA) as a second balancing indicator. These metrics were inspired by balance and motor control literature: SDLA reflects the extent of whole-body movement to maintain balance (Pai & Patton, 1997), while SDRA indicates the degree of hip strategy employed (Horak & Nashner, 1986).

2.3.3. Cycling vs e-scootering in obstacle avoidance

While SDLP and SDSA may measure the subject's performance in lateral control and SDLA and SDRA those in balancing and may be enough for the cruising and lane centering task, they do not disclose how well the avoidance task was performed. Therefore, for each subject and all obstacle avoidance tasks, we computed the number of crashes (NC), the minimum distance to the avoided obstacles (MinD), and the time at which the steering reversal, necessary to avoid the next obstacle, was performed in relation to the obstacle just avoided (TTR). These indicators were used to compare how well participants avoided obstacles depending on the vehicle they used. This analysis is intended to illustrate how task performance may be used to compare maneuverability across vehicles—a critical use case that makes use of the unique features of our simulator compared to the state-of-the-art.

2.3.4. Correlation analysis

Because lateral control and balancing influence each other, we computed correlation matrices for the four proposed performance indicators to assess potential redundancy. This analysis was performed separately for each vehicle across all tasks. Because 12 subjects joined the experiment and contributed one trial for each of the riding conditions, only correlation coefficients above 0.576 could be considered statistically significant.

2.3.5. Statistical description and analysis of the results

We summarized the statistical properties of the four performance indicators across tasks and vehicles. Four generalized linear mixed-effect models (GLMM) were created, one for each of the variables, to statistically verify the main effects of task (only cruising

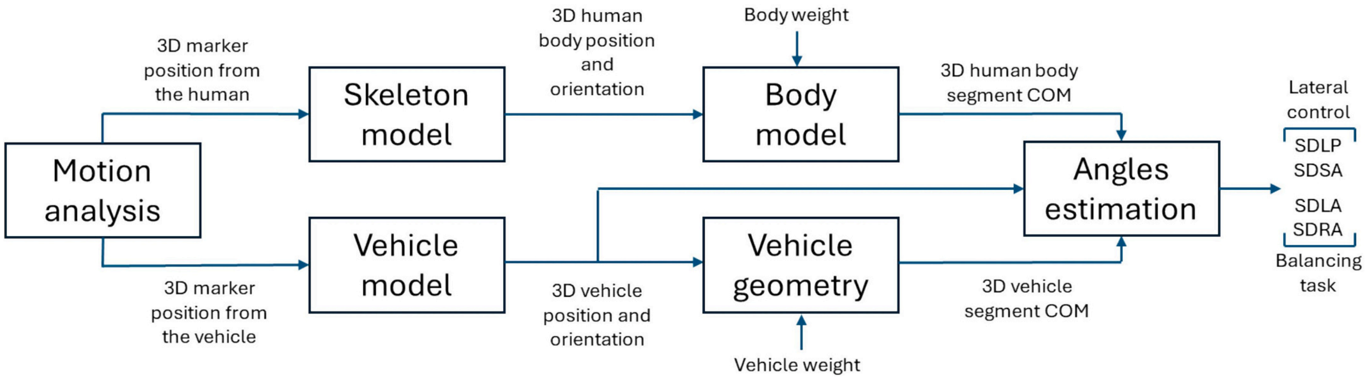

Fig. 4. – Data processing and analysis to estimate: standard deviations of 1) lane position (SDLP), 2) steering angle (SDSA), 3) lean angle of rider and vehicle combined (SDLA), and 4) relative angle between the upper and lower body in the lateral plane (SDRA).

and obstacle avoidance were considered), vehicle, and speed. Participant identification number (ID) was included as a random factor (Eq. 1).

$$Y_{ij} = \beta_0 + \beta_1\ \mathrm{Task}_i + \beta_2\ \mathrm{Speed}_i + \beta_3\ \mathrm{Vehicle}_i + \beta_4\ (\mathrm{Task} \times \mathrm{Speed})_i\ + \beta_5\ (\mathrm{Task} \times \mathrm{Vehicle})_i + \beta_6\ (\mathrm{Speed} \times \mathrm{Vehicle})_i\ + b_j + \epsilon_{ij} \tag{1}$$

Y_{ij} = dependent variable (SDLP, SDSA, SDLA, or SDRA) for observation i from participant j

- β_0 = intercept (reference condition: cruising, 6 km/h, bicycle)
- β_1 = main effect of Task (cruising vs. obstacle avoidance)
- β_2 = main effect of Speed (6 vs. 20 km/h)
- β_3 = main effect of Vehicle (bicycle vs. e-scooter)
- β_4 = interaction effect of Task × Speed
- β_5 = interaction effect of Task × Vehicle
- β_6 = interaction effect of Speed × Vehicle
- b_j = random intercept for participant j, where $b_j \sim N(0, \sigma_b^2)$
- ϵ_{ij} = residual error, where $\epsilon_{ij} \sim N(0, \sigma^2)$

The GLMM was primarily used to verify the indicators introduced in this new setup. Consequently, it seemed appropriate to include Task as a factor, even if the results might appear obvious once the indicators are confirmed. Similarly, we treated the center-lane task as a reference and excluded it from the model to maintain simplicity. Our goal with this statistical analysis was to verify the validity of the performance indicators rather than draw conclusions about lateral control or balance across different tasks or vehicles—an effort that may have required a larger number of participants. Statistical significance was set to α = 0.05 to follow common practice.

A simpler GLMM compared across cycling and e-scootering during obstacle avoidance (Eq. 2). In this case, the dependent variables were MinD and TTR.

$$Y_{ij} = \beta_0 + \beta_1\ \mathrm{Vehicle}_i + \beta_2\ \mathrm{Speed}_i + \beta_3\ (\mathrm{Speed} \times \mathrm{Vehicle})_i\ + b_j\ + \epsilon_{ij} \tag{2}$$

Y_{ij} = dependent variable (MinD and TTR) for observation i from participant j

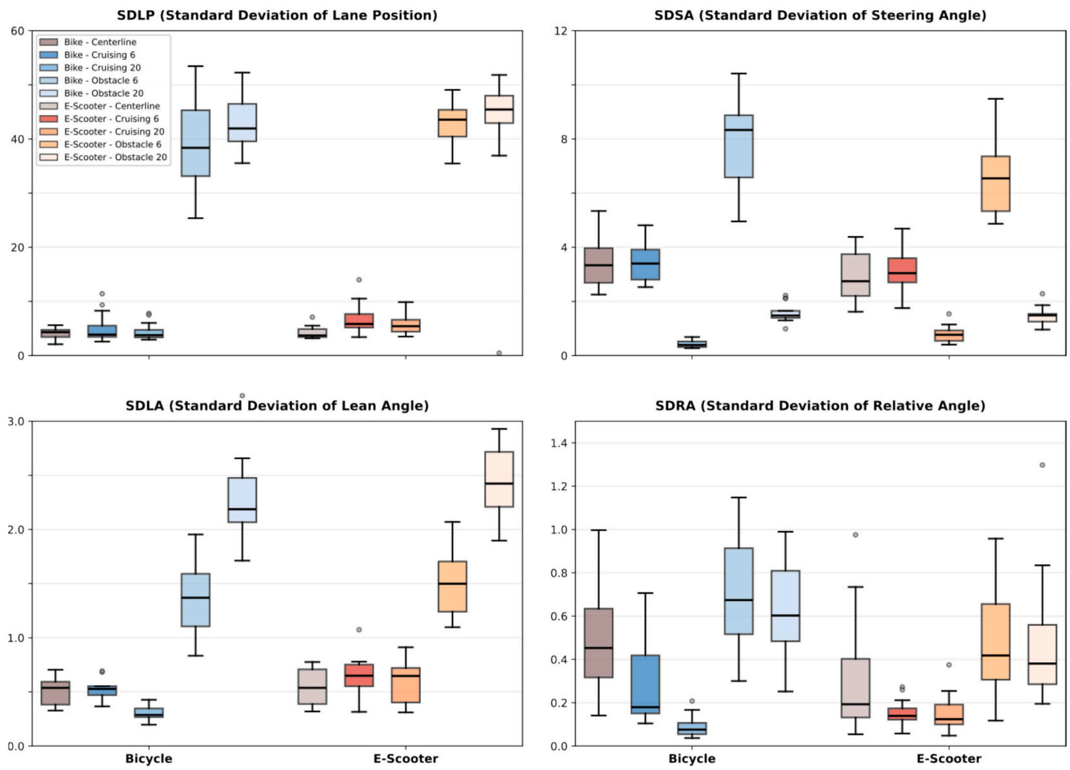

Fig. 5. – Comparison across tasks for all four performance indicators. Angles are expressed in degrees, SDLP in cm. The lane centering task is grayed as it presented as a reference and was not used for analysis. Box plots display the median value as a thick horizontal line, with boxes representing the 25th and 75th percentiles (Q1 and Q3). The interquartile range (IQR), defined as Q3 − Q1, was used to determine whiskers extending from Q1–1.5 × IQR to Q3 + 1.5 × IQR. Values beyond these whiskers were plotted as outliers.

- β_0 = intercept (reference condition: cruising, 6 km/h, bicycle)
- β_1 = main effect of Vehicle (cruising vs. obstacle avoidance)
- β_2 = main effect of Speed (6 vs. 20 km/h)
- β_3 = interaction effect of Vehicle × Speed
- b_j = random intercept for participant j, where $b_j \sim N(0, \sigma_b^2)$
- ϵ_{ij} = residual error, where $\epsilon_{ij} \sim N(0, \sigma^2)$

3. Results

3.1. Lateral control

As expected, SDLP was smallest during the lane-centering task, slightly larger while cruising, and substantially larger in the obstacle-avoidance task for both vehicles (Fig. 5A). This latest result was statistically significant in the GLMM model (Table 1). Increasing speed raised SDLP in the obstacle-avoidance task but reduced it during cruising (Fig. 5A), these results were close to statistical significance (both $p = 0.09$; Table 1).

At 6 km/h, SDSA was also lowest in the lane-centering task, moderately higher while cruising, and highest in obstacle avoidance. Again, the latter result was significant from the GLMM (Table 1). However, increasing speed significantly reduced SDSA across all tasks and both vehicles—a result that proved been statistically significant (Fig. 5B; Table 1).

3.2. Balancing task

The effects of task and speed on SDLA mirrored those observed for SDLP; however, speed had a stronger impact on increasing SDLA, particularly for the bicycle during obstacle avoidance (Fig. 5C). Beside confirming that Task had a statistically significant effect on SDLA, the GLMM pointed to a statistically significant difference between cycling and e-scootering at high speed in the cruising task. In fact, SDLA decreased for cycling but not for e-scootering as speed increased in the cruising task.

SDRA was generally higher when cycling than when e-scootering and was lowest during the cruising task (both results were statistically significant; Table 1). Increasing speed reduced SDRA overall, a statistically significant result (Table 1). Notably, SDRA values in the lane-centering task were nearly as high as those in obstacle avoidance (Fig. 5D).

Correlation analysis.

Performance indicators were generally weakly correlated, and the strength of these correlations varied considerably across tasks and vehicle types. Indicators tended to be less correlated for e-scootering compared to cycling (Fig. 6). Moreover, correlations declined as speed increased (Fig. 6). The strongest relationship was observed between SDLA and SDSA; however, this correlation was notably low when cruising on an e-scooter at 20 km/h.

3.3. Riding performance in obstacle avoidance

Crashing with a virtual obstacle was more likely when cycling (58; 12% crash rate) than when e-scootering (45; 9% crash rate). Higer speeds resulted in larger crash rates, especially for e-scootering (8% vs 11%). However, MinD was not significantly different between vehicles or speeds (Table 2). TTR became shorter as speed increased, a result that was expected from the protocol; however, the interaction between vehicle and speed was also significant (Table 2), showing that cyclists anticipated turning more so than e-scooterists.

3.4. Subjective rating of the riding simulator

Participants rated the overall simulator experience very highly, with a median score of 6 on a scale ranging from 5 to 7. Individual tasks were also rated favorably, with a median score of 6. The rating ranges varied slightly across tasks: lane-keeping tasks were rated between 5 and 7, whereas obstacle-avoidance tasks ranged from 3 to 7. Notably, only one participant rated the obstacle-avoidance task

Table 1
GLMM Analysis Results Summary for cruising vs. obstacle avoidance. The baseline condition is cruising with a bike at 6 km/h.

	SDLP		SDSA		SDLA		SDRA	
	β	p	β	p	β	p	β	p
Intercept	**47.82**	*	**3.44**	*	**0.50**	*	**0.29**	*
Task: obstacle avoidance	**350**	*	**4.43**	*	**0.90**	*	**0.43**	*
Speed: 20 km/h	−1.82	0.09	**−3.12**	*	−0.17	0.13	**−0.16**	**0.01**
Vehicle: *E*-scooter	20.37	0.20	−0.34	0.27	0.17	0.14	**−0.13**	**0.03**
Task × Speed	30.96	0.09	**−3.08**	*	**1.08**	*	0.05	0.48
Task × Vehicle	12.14	0.50	**−0.85**	**0.02**	−0.07	0.61	−0.11	0.09
Speed × Vehicle	−4.27	0.81	**0.91**	**0.01**	0.11	0.40	**0.14**	**0.04**

* $p < 0.001$.

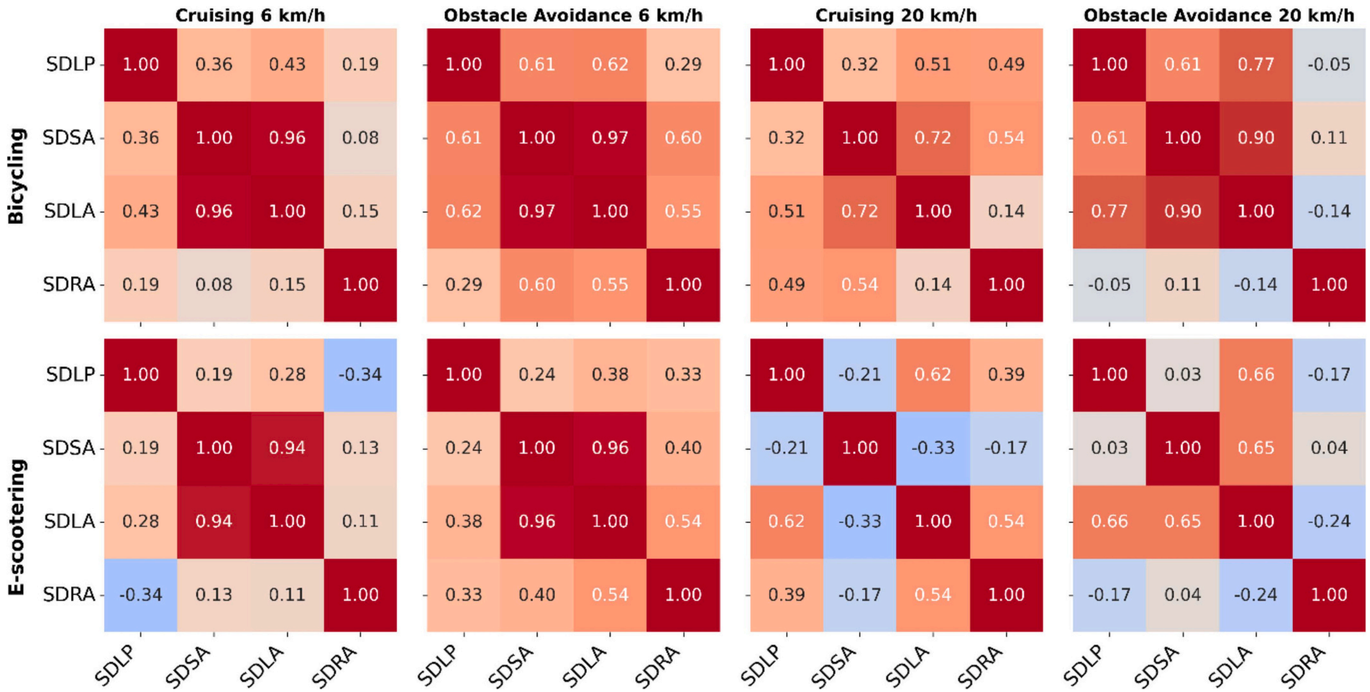

Fig. 6. – Correlation matrixes for all tasks: bicycling tasks at the top and e-scootering tasks at the bottom.

Table 2
GLMM Analysis Results Summary for cycling vs e-scootering. The baseline condition is cycling at 6 km/h.

	MinD		TTR	
	β	p	β	p
Intercept	**0.18**	*	**0.25**	*
Speed: 20 km/h	−0.01	0.37	**−0.28**	*
Vehicle: E-scooter	0.01	0.46	−0.04	0.45
Speed × Vehicle	0.01	0.56	**0.31**	*

* $p < 0.001$.

as 3, and none rated it as 4.

4. Discussion

This paper introduces a next-generation riding simulator that preserves the balancing task, is vehicle-agnostic, and allows riders full lateral control. The integration of these three features—novel and unique to this simulator—enables the study of human balance and vehicle control across a wide range of micromobility vehicles within a single facility, a feature unmatched by existing riding simulators.

Our methodological contribution lies not only in combining a large treadmill with stereophotogrammetry for real-time rendering of virtual traffic environments, but also in proposing a framework to assess maneuvering and balancing performance separately through four complementary indicators, largely inspired by prior research in traffic safety (Bowers et al., 2010; Hildreth et al., 2000; Louwerens et al., 1987) and neuroscience (Horak & Nashner, 1986; Pai & Patton, 1997). In this study, we verified all four indicators and demonstrated how they vary across different tasks and speeds. As expected, SDLP was greatest during obstacle avoidance and smallest when riders were instructed to maintain a centered position. SDSA complemented SDLP by revealing, for example, that reduced SDLP during lane centering was likely achieved through increased steering corrections. In other words, SDLP and SDSA exhibited patterns in the riding simulator consistent with those observed in driving simulators.

Assessing the balancing task required substantially more data processing and complexity than evaluating lateral control; in fact, it involved multiple models to estimate the COM of both the rider and vehicle components. This effort was necessary because, while previous research on bicycle dynamics inferred balance primarily from the frame roll angle (Moore et al., 2009), disregarding the rider's contribution would contradict findings in motor control research (Pai & Patton, 1997). Ultimately, we proposed a minimal set of parameters that capture overall body movement (SDLA) while also accounting for the ability to achieve balance through independent control of upper and lower body segments (SDRA). SDLA was sensitive to speed during obstacle avoidance but showed little variation between lane-centering and cruising tasks, regardless of speed. In contrast, SDRA complemented SDLA by clearly distinguishing between cruising and lane-centering and revealing notable differences between cycling and e-scootering. Specifically, cycling exhibited greater relative movement between upper and lower body compared to e-scootering, a pattern observed under all conditions except when cruising at high speed.

In addition, our correlation analysis indicates that the four proposed parameters are not redundant, suggesting that they complement each other in capturing the two key components—vehicle maneuvering and human balance—that our setup aimed to preserve and our metrics sought to measure. This finding is significant because the minimal set of parameters required to evaluate vehicle control and human balance on micromobility vehicles remains unknown, as does how this set might vary with differences in vehicle geometry and design features.

When avoiding obstacles, cyclists crashed more often than e-scooterists; as speed increased, cyclists also anticipated their steering maneuvers to avoid the next obstacle, a behavior that was not equally evident for e-scooterists. While the difference in wheelbases among the two vehicles may explain the necessity for bicyclists to increase their anticipatory control as speed increased to avoid obstacles, SDRA may help explain *how* the anticipatory control was achieved. In fact, the increased multi-segmental strategy (SDRA) found for cyclists but not for e-scooterists at higher speeds may be its root cause. While future studies may further explore the relation between multi-segmental strategy and anticipatory control, their potential relationship, that emerged in this study, may serve as an example of how understanding the balancing task may be crucial to compare performance across vehicles.

Although this simulator surpasses existing solutions in terms of balancing realism and its ability to accommodate virtually all micromobility vehicles (Table 3), it still presents several limitations beyond the further need for validation. Although preserving the

Table 3
– Comparison across riding simulators.

Simulator	Balancing task	Horizontal field of view	Lateral control	Longitudinal control	Vehicle
Ochel et al., 2025	On rollers	360°	Limited by the rollers	No	Bicycle
Stemmler et al., 2024[‡]	Not necessary	Up to 360°	Yes	Yes	Bicycle
Sporrel et al., 2025	Artificially recreated	180+ °	Yes	Yes	Bicycle
This paper	Real	30–40°	Max 2.5 m displacement	No	Any micromobility vehicle[†]

‡ This static bicycle simulator is representative of the majority of cycling simulators developed so far.
† Testing a monowheel or e-skates would create new challenges for this set-up; however, for e-scooters and bicycles any model would work.

balancing task and using real vehicles enhance validity (since both the balancing task and vehicle operation are physically real) the tasks performed in this study were not systematically compared with equivalent tasks conducted in real-world conditions. Moreover, while all twelve participants reported the simulator to be realistic, further validation of the simulator is still required. Another limitation is longitudinal control, braking in the current setup could lead to severe injuries. A potential solution is to leverage the motion analysis system to monitor the user's longitudinal position and incorporate this data into a feedback loop controlling treadmill speed. While efforts are underway to implement this feature, the delay in the feedback loop remains unknown. Consequently, the maximum braking force a user can apply before the treadmill fails to adjust its speed quickly enough to prevent a fall is still uncertain. Moreover, braking on a treadmill differs fundamentally from braking on a road, particularly when the vehicle's heading is not aligned with the treadmill's direction of motion. Consequently, automatically adjusting the treadmill speed may still prove impractical.

Future applications and developments of this and other riding simulators will help clarify how best to employ these tools across domains such as: 1) human factors research, (e.g., rider perception, reaction times, cognitive load, intoxication), 2) ADAS and automated features (e.g., interaction among AV and micromobility), 3) training & education, (e.g., skill acquisition, hazard awareness), 4) vehicle dynamics and controls, (e.g., how humans control and balance micromobility vehicles), 6) ergonomics & biomechanics, (e.g., posture analysis while riding, mounting/dismounting, falling), and 7) infrastructure design, (e.g., perceived safety and comfort of the built environment).

While the riding simulator presented in this paper is primarily intended for researchers working in the domains outlined above, it may also offer value to a range of other stakeholders, including governmental agencies and industry. In particular, the simulator has the potential to serve as a decision-support tool, allowing different infrastructure solutions to be evaluated and compared prior to real-world deployment. It may also function as a test facility for benchmarking prototype vehicles and intelligent safety systems, with the aim of improving performance and safety. For example, the simulator is currently being used to develop an intoxication-detection algorithm (Dozza & Rasch, 2026), namely a classifier designed to identify signatures of alcohol impairment from vehicle dynamics and to enable rental services to suspend or limit access for intoxicated riders. This use case is particularly exemplary for our riding simulator, as a high degree of realism in the balancing task is essential, while testing under real traffic conditions would be unethical.

5. Conclusions

By integrating a large treadmill with stereophotogrammetry, we enable virtual testing of micromobility vehicles without compromising the balancing task. We verified that the indicators SDLP and SDSA capture key aspects of lateral control for bicycles and e-scooters, while SDLA and SDRA provide insight into how riders maintain balance across different tasks and speeds. Although it remains unclear whether these are the optimal indicators for assessing vehicle control and balance or whether they generalize to all micromobility vehicles, we demonstrated that they are not redundant and, when combined, can distinguish among tasks, vehicle types, and speeds. Future work should focus on validation, developing more sophisticated metrics, enhancing simulator dynamics, immersion, and connectivity, and exploring additional riding tasks. Most importantly, further research is needed to determine how riding simulators can best support micromobility studies. In fact, while these simulators hold promises for advancing our understanding of human-vehicle control, intelligent transport systems, and infrastructure design, we still lack clear guidance on how to employ them effectively and do not know what level of realism is required to produce valid results.

Supplementary data to this article can be found online at https://doi.org/10.1016/j.trf.2026.103739.

CRediT authorship contribution statement

Marco Dozza: Writing – review & editing, Writing – original draft, Visualization, Validation, Supervision, Resources, Project administration, Methodology, Investigation, Funding acquisition, Formal analysis, Conceptualization. **Tianyou Li:** Writing – review & editing, Visualization, Software, Methodology, Data curation, Conceptualization. **Fredrik Bruzelius:** Writing – review & editing, Supervision, Resources, Methodology, Investigation, Conceptualization.

Declaration of competing interest

The authors declare that they have no known competing financial interests or personal relationships that could have appeared to influence the work reported in this paper.

Acknowledgements

This study and the development of the simulator presented in the study was made possible by the combined efforts from several research projects: e-Model, MicroSIM, and MinTOX sponsored by Chalmers and MicroTOX sponsored by VINNOVA. We would also like to acknowledge the support from Henrik Hörlin, Peter Bäckgren, and Kristina Henricson Briggs who greatly facilitated our access to the Tracks facilities at Chalmers Fuse. Large language models were used to revise the text of this manuscript; after that, the authors have reviewed the manuscript and take full responsibility for its content.

Data availability

Data will be made available on request.

References

Bowers, A. R., Mandel, A. J., Goldstein, R. B., & Peli, E. (2010). Driving with hemianopia, II: Lane position and steering in a driving simulator. *Investigative Ophthalmology & Visual Science, 51*(12), 6605–6613. https://doi.org/10.1167/IOVS.10-5310

Christoforou, Z., Kallianiotis, A., Athanasatos, A., Giannoulaki, M., Roumeliotis, S., & Gioldasis, C. (2026). *Development of an E-scooter simulator*. Lecture Notes in Mobility, Part F903 (pp. 104–109). https://doi.org/10.1007/978-3-031-88974-5_16/FIGURES/8.

Delp, S. L., Anderson, F. C., Arnold, A. S., Loan, P., Habib, A., John, C. T., … Thelen, D. G. (2007). OpenSim: Open-source software to create and analyze dynamic simulations of movement. *IEEE Transactions on Biomedical Engineering, 54*(11), 1940–1950.

Dialynas, G., Happee, R., & Schwab, A. L. (2019). Design and hardware selection for a bicycle simulator. *Mechanical Sciences, 10*(1), 1–10. https://doi.org/10.5194/ms-10-1-2019

Dozza, M., & Rasch, A. (2026). *Stöd till MinTOX : intelligenta system för berusningsdetektering i mikromobilitet*. . In *Skyltfonden*. Chalmers http://trafikverket.diva-portal.org/smash/get/diva2:2044758/FULLTEXT01.pdf

Hildreth, E. C. H., Beusmans, J. M., Boer, E. R., & Royden, C. S. (2000). From vision to action: Experiments and models of steering control during driving. *Donges, 26*(3), 1106–1132. https://doi.org/10.1037/0096-1523.26.3.1106

Horak, F. B., & Nashner, L. M. (1986). *Central programming of postural movements: Adaptation to altered support-surface configurations. 55* pp. 1369–1381). https://doi.org/10.1152/JN.1986.55.6.1369, 6.

Jafari, M., Persaud, B., & D'agostino, C. (2025). A hybrid structural equation modeling and fuzzy-set qualitative comparative analysis framework for using limited samples to relate cycling performance to behavioral traits. *Traffic Safety Res, 9*, Article e000095. https://doi.org/10.55329/qjgq4392

Louwerens, J. W., Gloerich, A. B. M., De Vries, G., Brookhuis, K. A., & O'Hanlon, J. F. (1987). The relationship between drivers' blood alcohol concentration (BAC) and actual driving performance during high speed travel. *Alcohol Drugs Traffic Saf, 86*, 183–186.

Lyu, W., Mun Lee, Y., Uzondu, C., Madigan, R., Gonçalves, R. C., Garcia de Pedro, J., … Merat, N. (2024). A distributed simulation study to investigate pedestrians' road-crossing decisions and head movements in response to different vehicle kinematics in mixed traffic. *Transportation Research Part F: Traffic Psychology and Behaviour, 104*, 1–14. https://doi.org/10.1016/J.TRF.2024.04.023

Markkula, G., Benderius, O., Wolff, K., & Wahde, M. (2013). Effects of experience and electronic stability control on low friction collision avoidance in a truck driving simulator. *Accident Analysis & Prevention, 50*, 1266–1277. https://doi.org/10.1016/J.AAP.2012.09.035

Merat, N., Jamson, A. H., Lai, F. C. H., Daly, M., & Carsten, O. M. J. (2014). Transition to manual: Driver behaviour when resuming control from a highly automated vehicle. *Transportation Research Part F: Traffic Psychology and Behaviour, 27*(PB), 274–282. https://doi.org/10.1016/J.TRF.2014.09.005

MicroVRide. (2025). https://www.ri.se/en/expertise-areas/projects/microvride-virtual-reality-micromobility-simulator. In *Web* https://www.ri.se/en/expertise-areas/projects/microvride-virtual-reality-micromobility-simulator.

Mohammadi, A., Bianchi Piccinini, G., & Dozza, M. (2023). How do cyclists interact with motorized vehicles at unsignalized intersections? Modeling cyclists' yielding behavior using naturalistic data. *Accident Analysis & Prevention, 190*, Article 107156. https://doi.org/10.1016/J.AAP.2023.107156

Moore, J. K., Kooijman, J. D. G., & Schwab, A. L. (2009). *Rider Motion Identification During Normal Bicycling by Means of Principal Component Analysis*. Multibody Dynamics. http://bicycle.tudelft.nl.

Morando, A., Victor, T., Bengler, K., & Dozza, M. (2021). Users' response to critical situations in automated driving: Rear-ends, sideswipes, and false warnings. *IEEE Transactions on Intelligent Transportation Systems, 22*(5), 2809–2822. https://doi.org/10.1109/TITS.2020.2975429

Ochel, L., Saparia, S., Weidel, M., Johansson, A., & Kircher, K. (2025). How we roll - realistic cycling simulator for Behavioural Research, 53–58. https://proceedings.driving-simulation.org/proceeding/dsc-2025/how-we-roll-realistic-cycling-simulator-for-behavioural-research

O'Hern, S., & Estgfaeller, N. (2020). A scientometric review of powered micromobility. *Sustainability, 12*(22), 9505.

Pai, Y. C., & Patton, J. (1997). Center of mass velocity-position predictions for balance control. *Journal of Biomechanics, 30*(4), 347–354. https://doi.org/10.1016/S0021-9290(96)00165-0

Plumert, J. M., Kearney, J. K., Cremer, J. F., Recker, K. M., & Strutt, J. (2010). Changes in children's perception-action tuning over short time scales: Bicycling across traffic-filled intersections in a virtual environment. *Journal of Experimental Child Psychology, 108*(2), 322. https://doi.org/10.1016/J.JECP.2010.07.005

Rajagopal, A., Dembia, C. L., DeMers, M. S., Delp, D. D., Hicks, J. L., & Delp, S. L. (2016). Full-body musculoskeletal model for muscle-driven simulation of human gait. *IEEE Transactions on Biomedical Engineering, 63*(10), 2068–2079.

Sandt, L., & Owens, J. M. (2017). *Discussion guide for automated and connected vehicles, pedestrians, and bicyclists*.

Shoman, M. M., & Imine, H. (2021). Bicycle simulator improvement and validation. *IEEE Access, 9*, 55063–55076. https://doi.org/10.1109/ACCESS.2021.3071214

Sporrel, B., PenaPerez, N., Vallery, H., Schwab, A., & De Waard, D. (2025). *Validation of a high-fidelity Fytssimulator with an on-road cycling task*. Oslo: Proceeding of the international cycling safety conference.

Stemmler, T., Schoch, S., Hornung-Prähauser, V., Hollauf, E., Claudia, L.-B., Schaffner, D., Haiderer, N., Gantenbein, S., & van Eggermond, M. (2024). *Sichere und effiziente S-Pedelec-Infrastruktur S-ESPIN*.

Von Sawitzky, T., Grauschopf, T., & Riener, A. (2022). Hazard notifications for cyclists: Comparison of awareness message modalities in a mixed reality study. *International Conference on Intelligent User Interfaces, Proceedings IUI, 22*, 310–322. https://doi.org/10.1145/3490099.3511127

Weir, D. H. (2010). Application of a driving simulator to the development of in-vehicle human–machine-interfaces. *IATSS Research, 34*(1), 16–21. https://doi.org/10.1016/J.IATSSR.2010.06.005